Received: 23 March 2020 | Revised: 10 June 2020 | Accepted: 14 June 2020

DOI: 10.1002/app.49726

ARTICLE

Applied Polymer Science WILEY

Self-adhesive plasticized regenerated silk on poly (3-hydroxybutyrate-*co*-3-hydroxyvalerate) for bio-piezoelectric force sensor and microwave circuit design

Silvia Bittolo Bon[1,2] | **Luca Valentini**[1,2] | **Micaela Degli Esposti**[2,3] | **Davide Morselli**[2,3] | **Paola Fabbri**[2,3] | **Valentina Palazzi**[4] | **Paolo Mezzanotte**[4] | **Luca Roselli**[4]

[1]Dipartimento di Ingegneria Civile e Ambientale, Università degli Studi di Perugia, Terni, Italy

[2]Italian Consortium for Science and Technology of Materials (INSTM), Firenze, Italy

[3]Department of Civil, Chemical, Environmental, and Materials Engineering (DICAM), Università di Bologna, Bologna, Italy

[4]Dipartimento di Ingegneria, Università degli Studi di Perugia, Perugia, Italy

Correspondence
Luca Valentini, Dipartimento di Ingegneria Civile e Ambientale, Università di Perugia, Terni, Italy.
Email: luca.valentini@unipg.it

Funding information
Ministero dell'Istruzione, dell'Università e della Ricerca, Grant/Award Number: 2017FWC3WC_003

Abstract

This study shows that regenerated silk (RS), a natural biodegradable and biocompatible polymer, can behave as a self-adhesive thermoplastic material with multifunctional properties. In particular, Ca ions-plasticized RS hybrids with gold nanorods have been produced. It has been found that at mild conditions of temperature and pressure, RS hybrids undergo to the loss of the β-sheet content and forms a tough self-adhesive material on poly(3-hydroxybutyrate-*co*-3-hydroxyvalerate) (PHBV) substrate. The structure-dependent piezoelectricity of such RS adhesives on PHBV films was investigated and it was demonstrated that this forms a RS/PHBV piezoelectric sensor that can be used for the monitoring of force. The constitutive parameters (i.e., permittivity and loss tangent) of both PHBV and RS/PHBV were measured in view of their use as dielectric substrates in microwave circuit design. Being fully made of biodegradable and biocompatible materials, this self-adhesive material can be used in tissue engineering for different applications.

KEYWORDS

adhesives, biopolymers and renewable polymers, mechanical properties, sensors and actuators

1 | INTRODUCTION

Silkworm silk and silk fibroin are natural biopolymers.[1–3] Natural silk is a semicrystalline material that is difficult to process as a traditional polymer; for this reason, different solvent based methods have been developed to extract solubilized silk fibroin from natural silk.[4–7] Ca-modified regenerated silk (RS)/gold nanorods (GNR) hybrids, for example, have been engineered to be a material with high elongation at break and high water absorption,[8] which was shown to be crucial for sealing anastomotic leaks.[9]

Hot pressing is a technique that is generally used to couple two different materials that are welded to the interface due to the effect of heat.[10] In general, this technique is typical of thermoplastic polymeric materials.[11] So the combination of two polymers depends on the modification of their structure at the interface once subjected to heat. In order to obtain the thermal welding with RS, it is therefore necessary that it behaves like a thermoplastic material. This property is not easy to obtain because RS is not intrinsically a thermoplastic material. In this work we observed that subjecting the RS to specific conditions of temperature

and pressure, we are able to obtain a reduction of the crystalline fraction, which leads to remarkable self-adhesive properties.

RS is also known as a material with functional properties.[12,13] Among these properties, the possibility of creating interfaces with soft tissues and monitoring biological forces push the attention to materials with piezoelectric properties.[14] Such materials can be used as self-powered force sensors.[15] Unfortunately, most of them (i.e., lead zirconate titanate and polyvinylidene difluoride) are toxic and nonbiodegradable. Piezoelectric materials have crystal structures with a low degree of symmetry.[16] Silk fibroin, being a natural polymer with a tunable crystallinity, has an intrinsic piezoelectricity that depends on the processing parameters including stretching, and post-synthesis treatments.[16]

Poly(3-hydroxybutyrate-*co*-3-hydroxyvalerate) (PHBV) is the copolymer of the well-known poly(3-hydroxybutyrate) (PHB) and due to its biocompatibility properties it is largely used in tissue engineering.[17] Recently, the polyhydroxyalkanoates have been also indicated by the European commission as one of top 20 most innovative bio-based products.[18] This fully bio-based class of polymers is typically obtained through a fermentation process that uses, as feedstock, sugar beets and/or canes agro-wastes.[19] Moreover, PHBV is highly biodegradable[20] and bioresorbable.[21,22] These biodegradable polyesters showed piezoelectric properties[23] with a piezoelectric coefficient of PHBV that was used to induce bone reformation.[24] PHBV also showed a piezoelectric relaxation around the glass transition temperature.[25]

These materials can be also exploited in the field of with electronics, forming self-powering bio-based fully integrated systems to enable many applications within the emerging ICT eco-systems called internet of things.[26] These applications span over many areas and require highly eco-friendly disposable electronics (biodegradable, recyclable, and even compostable), such as monitoring monuments, distributed sensing in agriculture, prompt massive monitoring in rescue and harsh areas, where the recovery of sensors and electronics could be difficult and thus detrimental if composed of nonbiodegradable components.

Here, we present a method for RS thermal processing and assessment of a piezoelectric RS/PHBV interface to create a biodegradable force sensor. It could gain attention for monitoring biological forces and the application of the electrical stimulation in a biological system for tissue engineering. In this regard we employed in this study gold nanoparticles stabilized with a positively charged surfactant (cetyltrimethylammonium bromide, CTAB) according to recent studies that have demonstrated both the intracellular biodegradation of gold nanoparticles[27] and the recrystallization effect of CTAB in piezoelectric polymers.[28]

The new proposed hybrid biopolymers are also characterized electromagnetically to enable the design of the radiofrequency circuit components needed to acquire and communicate the sensor information.

2 | EXPERIMENTS

2.1 | Materials

Sodium hydrogen carbonate ($NaHCO_3$), calcium chloride ($CaCl_2$), formic acid, chloroform, GNR colloidal suspension stabilized in CTAB (diameter × length, 10 nm × 38 nm, ± 10%) and PHBV custom grade were supplied by Sigma-Aldrich. Liquid crystal rubber with catalyst were purchased from PROCHIMA.

2.2 | Materials preparation

B. mori cocoons were degummed according to a procedure reported elsewhere[9]: briefly they were boiled in $NaHCO_3$ at 100°C for 30 min, rinsed in deionized water. The process has been repeated a second time and the degummed silk was then left to evaporate in dry air at room temperature. The degummed silk was added to a $CaCl_2$/formic acid solution according to a procedure reported in reference 13. Three solutions with different silk:$CaCl_2$ weight ratios (i.e., 90:10, 80:20, and 70:30) were obtained. 1 ml of GNRs was added to 1 mL of RS solution and mixed at 6°C. The solution was stirred for 30 min. The solutions were deposited onto a polystyrene dish (5 cm diameter) at room temperature and left to evaporate the solvent for 8–12 h. Finally, it was heated at 60°C for 2 h to remove the residual solvent. Films with a thickness of approx. 100 μm were obtained. RS films with GNR are named 90:10 + GNR, 80:20 + GNR and 70:30 + GNR respectively.

Films of PHBV with thickness of approx and 300 μm were prepared by solvent-casting of a chloroform/polymer solution of 20 mg/ml in a Petri dish with a diameter of 15 cm (representative image in Figure S1). The used PHBV was previously purified following the procedure described elsewhere[22] in order to remove all the residues derived from biotechnological production process. Purified PHBV was characterized by proton nuclear magnetic resonance (^{1}H-NMR) and gel permeation chromatography (GPC) (experimental details in supporting information) before starting the device fabrication. The obtained results are shown in Figure S2 and summarized in Table **S1** of the supporting information file.

2.3 | Device fabrication

The RS and hybrid RS films were then hot pressed on PHBV substrate at 60 kPa and 95°C for 30 s. After hot pressing, these samples, named thereinafter thermal annealed (TA) films, were cooled to room temperature and used for further characterizations.

The piezoelectric device was fabricated as reported elsewhere.[9] Briefly, the RS/PHBV film was stick onto a bottom carbon tape electrode, then a carbon tape was attached to the top side. After that, Cu wires were attached to the bottom and top sides of the carbon tape using Ag paste (Scheme 1(a,b)). Finally, the device was encapsulated in silicone rubber obtained by mixing liquid crystal rubber with catalyst. The two components were mixed in 1:1 weight ratio. The polyaddition reaction occurs at 25°C and was completed in 12 h. Silicone wrapping is used to protect the device from humidity (Scheme 1(a)).

2.4 | Materials characterizations

The thermal behavior of the used polymeric films was evaluated by differential scanning calorimetry (DSC) on a Q10 (TA Instruments) equipped with a discovery refrigerated cooling system (RCS90, TA Instruments). Specifically, approximately 10 mg of each sample were placed into aluminum pans and subjected to two types of heating cycles. In the first the sample was investigated from −10 to +200°C with heating rate of 10°C/min. This scan was used for determining the temperature that could be used for the hot pressing in order to avoid the thermal degradation. The second was an isothermal cycle at 110°C for 10 min in order to simulate the hot-pressing conditions used to make the device (as described in Section 2.3). In both analyses the DSC cell was purged with a dry nitrogen flow (50 ml/min). Before the measurements the system was calibrated both in temperature and enthalpy with Indium standard. The obtained thermograms were processed with TA Universal Analysis 2000.

The modification in the structure of the RS due to the hot pressing was evaluated by Fourier transform infrared spectroscopy (FTIR, Jasco FT/IR 615, USA) (see supporting information section).

The mechanical properties of the films were measured accordingly to previous studies,[8,13] with a tensile testing machine (Lloyd Instr. LR30K, UK). Rectangular shape samples (1.5 cm × 3 cm × 100 μm) were stretched with a strain rate of 5 mm/min using a 500 N load cell. The

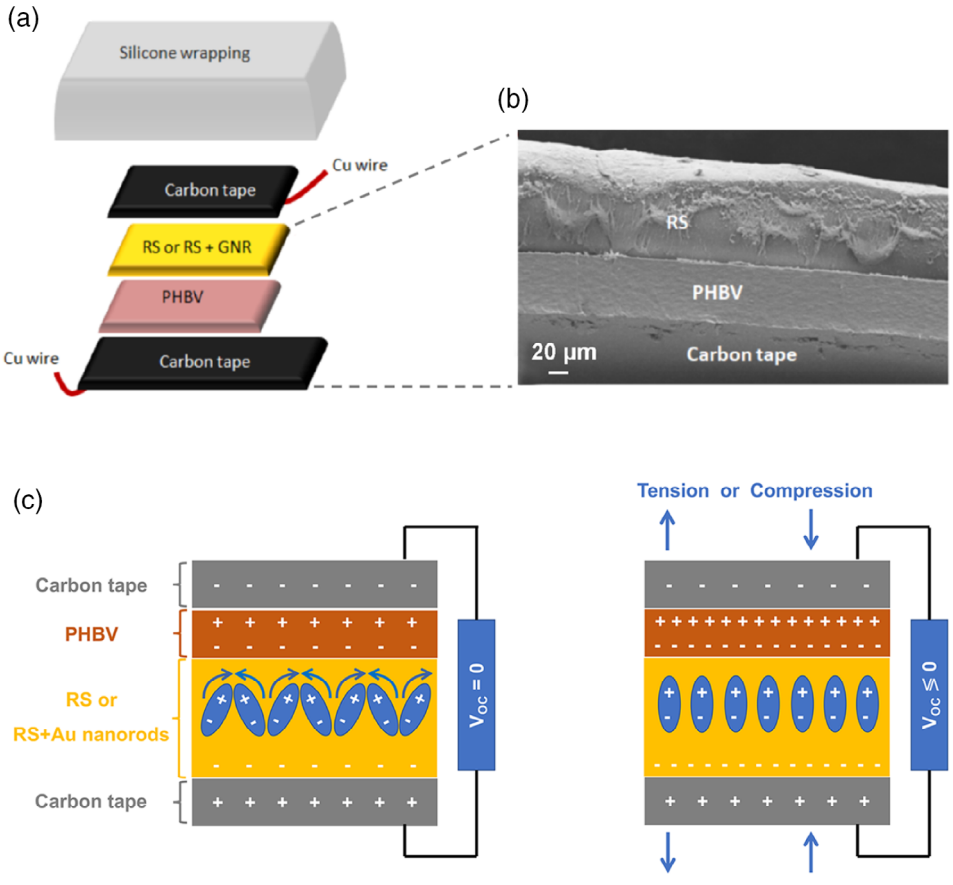

SCHEME 1 (a) Schematic representation of piezoelectric device fabrication, (b) Cross-sectional field emission scanning electron microscopy (FESEM) view of 90:10 RS-GNR/PHBV sample, and (c) Schematic representation of cross-section of the piezoelectric device and related working principle. GNR, gold nanorods; PHBV, poly(3-hydroxybutyrate-*co*-3-hydroxyvalerate) [Color figure can be viewed at wileyonlinelibrary.com]

mechanical characteristics (i.e., Young's modulus, tensile strength, and toughness) were then calculated from the stress–strain curves reported in Figure S3 (the results were the average values from at least three measurements for each composition). The tensile strength was measured with two films of PHBV that were adhered by hot pressing with RS in between and determined by tensile test dividing the maximum force by the adhesion area. Adhesion areas of 9 mm × 9 mm were considered with a strain rate of 5 mm/min (the results were the average values from at least three measurements for each composition).

The piezoelectric output of the devices was measured applying an external force of 5 N at a frequency of 1 Hz. The open circuit voltage values were monitored using a computer controlled Keithley 4200 source measure unit. For the static measurements, different weights were positioned on the sensor surface and the output signal under external forces (up to 1 N) was recorded (see Supporting Information and Figure S4).

2.5 | Electromagnetic characterization

The developed biopolymers are electromagnetically characterized at microwave frequencies using microstrip *T* resonators. The *T* resonator consists of a shunt open-circuited stub connected to a transmission line, which resonates when its length *(l)* is equal to integer multiplies of a quarter wavelength:

$$l = n \cdot (1/4) \cdot (\lambda_g), \quad (1)$$

where λ_g is the wavelength on the microstrip line and n is the order of resonance (n = 1,3,5,...).

The metal traces of the circuit are realized using the metal adhesive laminate technique.[26] The technique consists of shaping a copper adhesive laminate with photolithography. This way, high-resolution and high-conductivity metal traces are obtained (the conductivity

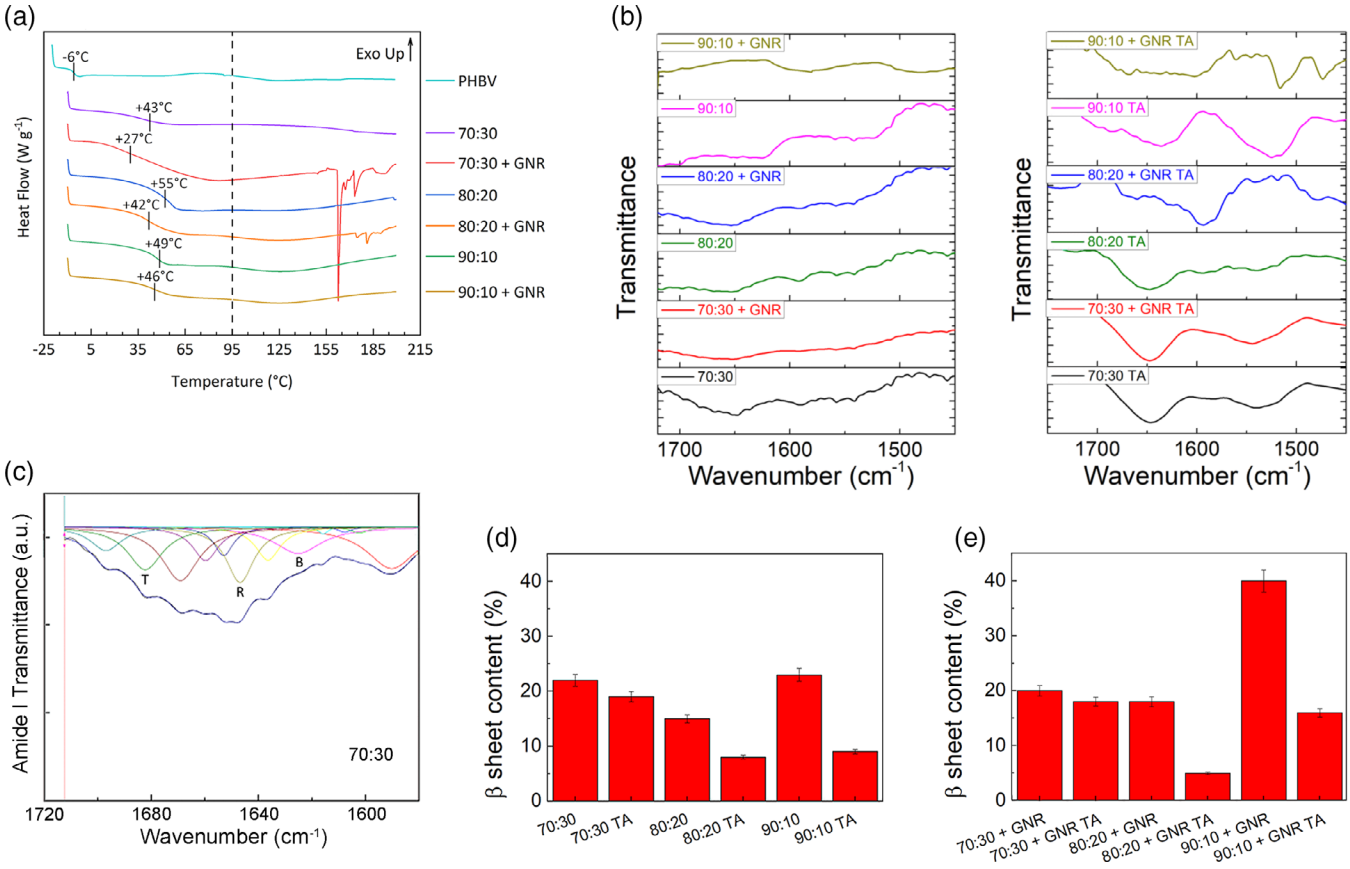

FIGURE 1 (a) DSC curves for all materials used for the device fabrication. Dashed line indicates the used temperature for the hot-pressing (95°C). Measured glass transition temperatures of the analyzed materials are reported on each thermogram. (b) FTIR spectra of RS and RS-GNR films before and after thermal annealing (TA), respectively. (c) Deconvolution of the amide I band for the 70:30 RS sample, as representative. The colored lines represent the amide I band components, which are indicated as β-sheets (B), random coils (R), and turns (T), respectively. β-sheets content of (d) RS, and (e) RS-GNR films before and after thermal annealing (TA) under gentle pressure (60 kPa), respectively. DSC, differential scanning calorimetry; FTIR, Fourier transform infrared spectroscopy; GNR, gold nanorods; RS, regenerated silk; TA, thermal annealing [Color figure can be viewed at wileyonlinelibrary.com]

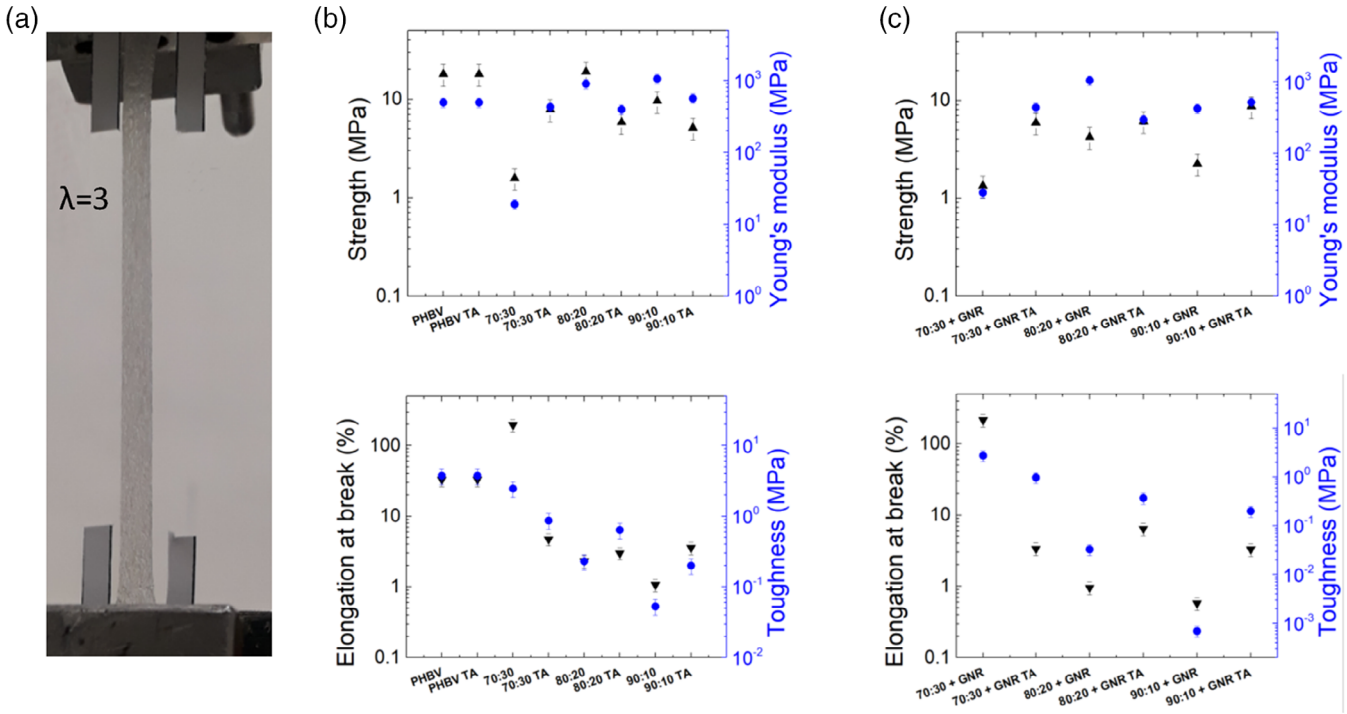

FIGURE 2 (a) Photograph of the 70:30 RS-GNR film stretched three times the original length. Effect of thermal annealing (TA) during the hot-pressing process on strength, modulus, elongation at break and toughness on the (b) RS, and (c) RS hybrid films, respectively. The mechanical properties of PHBV and thermally annealed PHBV (PHBV TA) are reported for comparison purpose. PHBV, poly(3-hydroxybutyrate-*co*-3-hydroxyvalerate); RS, regenerated silk; TA, thermal annealing [Color figure can be viewed at wileyonlinelibrary.com]

of bulk copper is 5.8×10^7 S/m), which are essential features to realize microwave circuits. The obtained metal pattern is then transferred to the substrates to be characterized using a sacrificial layer. The adhesion between the metal pattern and the substrate is guaranteed by the acrylic glue layer placed under the adhesive metal layer. The thickness of the metal layer is about 35 μm and the thickness of the glue is about 30 μm. The permittivity of the glue, equal to 2.4, is measured with a capacitance meter. The ground plane of the microstrip line is obtained sticking a piece of copper adhesive laminate on the other side of the substrate. The scattering parameters of the *T* resonators realized on the materials under test are measured with a vector network analyzer. The scattering parameters of the resonators are measured in the frequency range 1–40 GHz.

The *T*-resonator geometry is designed and simulated with a full-wave CAD (i.e., CST studio suite). The simulated reflection and transmission coefficients of the circuit are matched to the measured scattering parameters of the circuit in correspondence with the resonant frequencies by iterative refinement of the permittivity and loss tangent. For simplicity, the glue is assumed to be lossless, and all circuit losses are assigned to the material under test. Due to the reduced thickness of the glue with respect to the materials under test, this assumption has a negligible impact on the results.

3 | RESULTS AND DISCUSSION

The described method allowed us to produce thermally stable films. In particular, as shown by DSC thermograms in Figure 1(a), no peak due to thermal degradation processes of the used polymers can be detected nearby the selected temperature for hot-pressing. Only samples 70:30 + GNR and 80:20 + GNR show peaks between 165 and 190°C, which can be tentatively associate to melting transitions of a crystalline phase, which formation is induced by the presence of GNR and high content of Ca ions. However, for both samples, the peaks are in a temperature range remarkably higher than 95°C used for joining the two polymeric films, thus ensuring no thermal degradation phenomena during the hot-pressing step. This was further confirmed by isothermal DSC investigations (see thermograms in Figure S5). In fact, even though the isothermal tests were carried out in harsher conditions (temperature and time) than that one's actually used during the hot-pressing procedure, the thermograms do not show any peak due to

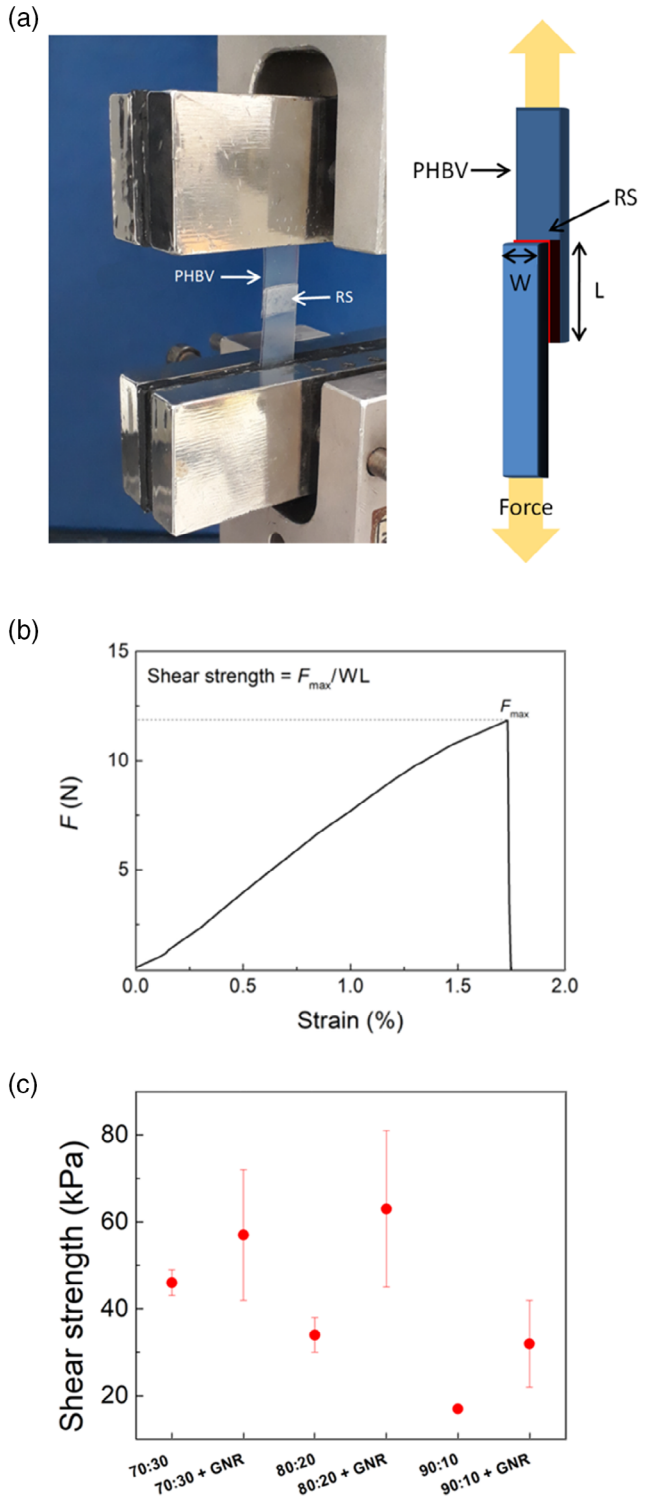

FIGURE 3 (a) Setup for measurement of adhesive strength; *L*, length; *W*, width. (b) Representative force-strain of the shear measurement in order to calculate the shear strength, *F*, force; F_{max}, maximum force in lap-shear. (c) Shear strength values of RS and hybrid RS thermal annealed samples, respectively. RS, regenerated silk; TA, thermal annealing [Color figure can be viewed at wileyonlinelibrary.com]

degradations or phase transitions. Furthermore, crystallinity changes of the films upon hot pressing were then investigated by FTIR (Figure 1(b,c)). The deconvolution of the amide I band provides an estimation of β-sheet structure in the RS and RS-GNR films that is reported in Figure 1(d,e).[29] Upon hot-pressing process, the FTIR analysis revealed also a reduction of the β-sheet structure in the samples with increased silk fibroin fraction. While the addition of GNR generally increases the crystalline fraction of RS instead comparing the FTIR spectra of Figure 1(b,c) with that recorded on CTAB GNRs (Figure S6), we did not record any chemical interaction between gold nanoparticles and silk.

The mechanical properties of the fabricated silk-based samples were characterized throughout tensile test. The obtained results, reported in Figure 2, are in accordance with previous studies.[30,31] In fact, as the calcium chloride content increases, the plasticization of the RS is accentuated, resulting in a stretchable material (Figure 2(a)). The Ca^{2+} ions have the capability to capture the humidity from the environment inducing a plasticizing effect on this polymeric material.[30] Figure 2(b,c) also show that the toughness of the as prepared samples generally increases after hot-pressing. In particular, while the tensile strength data do not show any trend upon the addition of GNR (i. e., the tensile strength value for 70:30 + GNR TA is ~8 MPa, while for 80:20 + GNR TA is 5 MPa and 12 MPa for 90:10 + GNR TA), the addition of GNR generally improves the elongation at break resulting in RS hybrid samples with improved toughness. Furthermore, as shown by DSC results (Figure 1(a)), the thermal degradation of the samples can be excluded as result of the thermal treatment, whereas the material becomes soft to allow thermal adhesion on designed substrates. DSC curves (Figure 1(a)) reveal indeed the typical thermal jump associated to the transition from the glassy to rubbery state. All samples showed a glass transition temperature (T_g) lower than 95°C used for the hot-pressing (Figure 1(a)), thus suggesting that during this process both materials are in the rubbery state.

To evaluate the adhesion of the RS and RS hybrids on PHBV, we measure the shear strength by lap-shear test (Figure 3(a)). The adhesion test verifies that RS and RS hybrids can adhere to PHBV films upon the application of heat and gentle pressure (60 kPa) for 30 s (Figure 3(b) and Supplementary Video). The obtained results for RS and RS hybrids (Figure 3(c)) demonstrate adhesion performance comparable to the shear strength of commercial adhesives (Histoacryl ≈ 100 kPa, Coseal ≈ 25 kPa, DuraSeal ≈ 12 kPa,

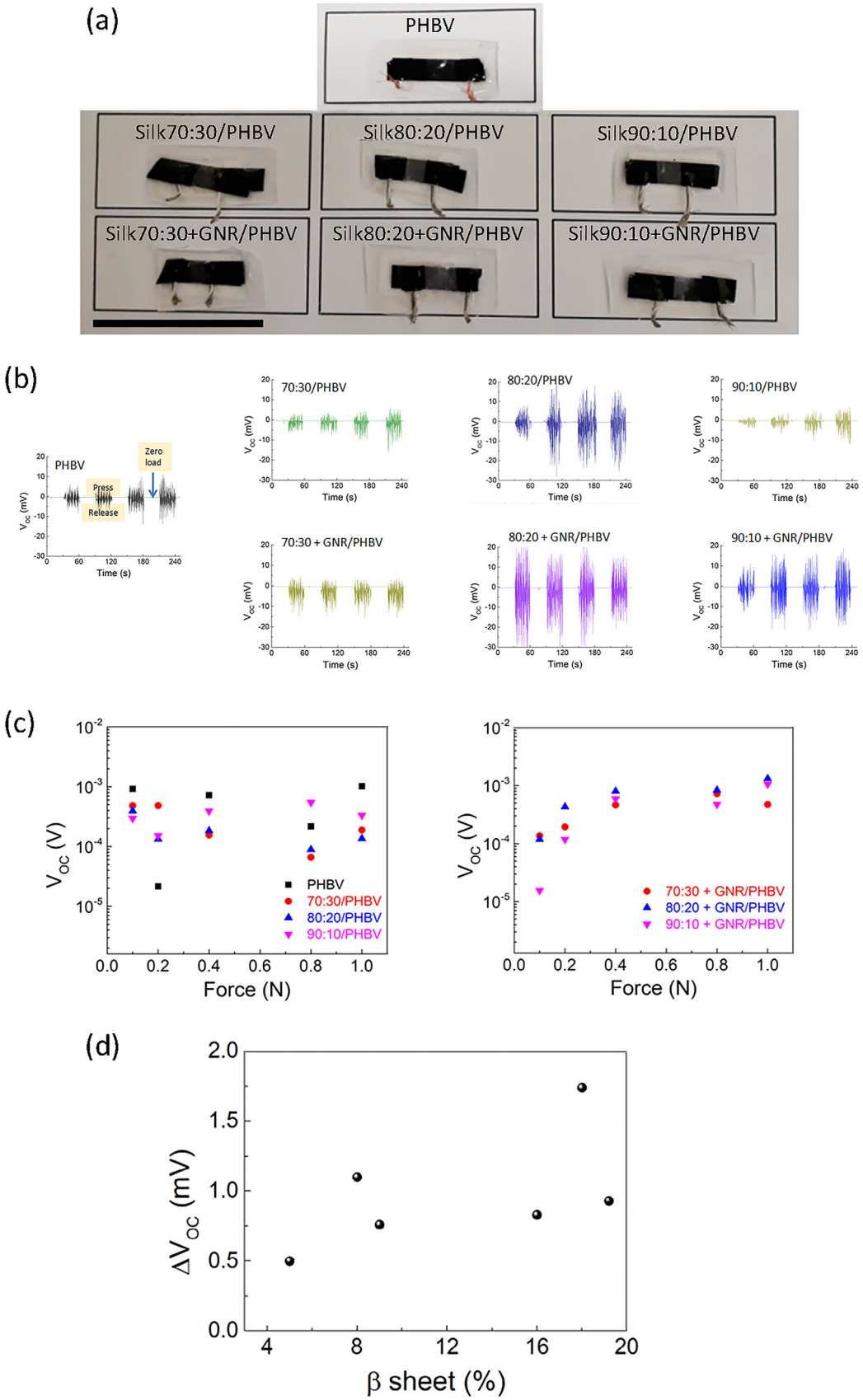

FIGURE 4 (a) Photographs of the piezoelectric devices fabricated. The scale bar indicates 20 mm. (b) The generated output voltage of piezoelectric devices fabricated with PHBV and RS-GNR/PHBV films with different Ca^{2+} content, subjected to repetitive loading and releasing pressure (frequency 1 Hz), (c) Output voltage signals of piezoelectric PHBV, RS/PHBV and RS-GNR/PHBV sensors as a function of different input of force, and (d) Variation of the open circuit voltage (V_{OC}) as a function of RS β-sheet content of the samples reported on the panel *b*. GNR, gold nanorods; PHBV, poly(3-hydroxybutyrate-*co*-3-hydroxyvalerate); RS, regenerated silk [Color figure can be viewed at wileyonlinelibrary.com]

Tisseel ≈ 12 kPa, and Tegaderm ≈ 50 kPa).[32–35] Moreover, it can be noticed that the presence of GNR leads to an overall increase of the shear strength for achieving the detachment of the two films. In particular, a shear strength of approximately 60 kPa was obtained for the sample 80:20 + GNR that showed the best adhesion, but with a pressure application time that is significantly shorter than that one typically required by commercially available adhesives to establish the adhesion (i.e., 5–30 min).

After verifying the adhesive properties of the RS and RS hybrids, we fabricated a piezoelectric force sensor by using self-adhering RS and RS hybrids on PHBV, carbon tape electrodes, and encapsulating silicone (Scheme 1(a) and Figure 4(a)).

Figure 4(b) shows open-circuit voltage signals of RS and RS-GNR films thermally coupled with PHBV, measured with 1 Hz variation of the applied load. The generated outputs from different RS/PHBV samples do not show a clear trend under different loads. On the contrary, the data collected from the RS-GNR/PHBV samples have a larger output signal and respect to the bio-piezoelectric PHBV-based force sensor, this device exhibits a response that increases with the applied load (Figure 4(b,c)). The output voltages reported in Figure 4(c) were calculated by applying a constant load at different time intervals (i. e., 20, 40, 60 and 80 s) and recording the signal that was mediated between the maximum and minimum value as reported in the Figure S7.

Figure 4(d) shows the variation (the difference between the press and release output signals) of the open circuit voltages of the samples reported in Figure 4(b) as a function of their respective RS β-sheet content; in general it was found that there is an increase of the piezoelectric performance with increasing the β-sheet content. Finally, measurements of the short circuit current (Isc) showed a behavior (Figure S8) that is not dependent by the polarity.

The structural origin of the piezoelectricity of silk was explained on the combination effect of content and orientation of β-sheets crystallinity.[16] Accordingly to that study in our case,[16] GNR addition to RS did result in a significant improvement in RS piezoelectricity as compared with RS/PHBV samples, in view of the presented results (Figure 4(d)), RS-GNR/PHBV piezoelectricity may be explained by polarization of in plane oriented β-sheet that could results in rubbering and formation of amide dipoles.[16] Thus, the working principle[36] is based on electrostatic induction: the application of mechanical pressure changes the electric field distribution of RS, and the PHBV generates at the interface charges with opposite polarities developing potential mismatch between two electrodes for electron transfer to an external circuit (as schematically shown in Scheme 1(c)).

Finally, permittivity and loss tangent of PHBV and RS-GNR/PHBV films are measured with the T-resonator method in order to investigate the electromagnetic properties. In particular, we tested the materials more promising in terms of piezoelectricity, which are the 80:20 + GNR/PHBV and 90:10 + GNR/PHBV samples. A representative picture of the fabricated resonator prototypes based on PHBV and on two samples of RS-GNR/PHBV films is shown in Figure 5(a). Figure 5(b) shows the PHBV sample connected to two end-launch connectors from Southwest used to connect the microstrip circuit to the vector network analyzer (model N5230A from Agilent Technologies). The cross-section of the microstrip circuit is shown in Figure 5(c).

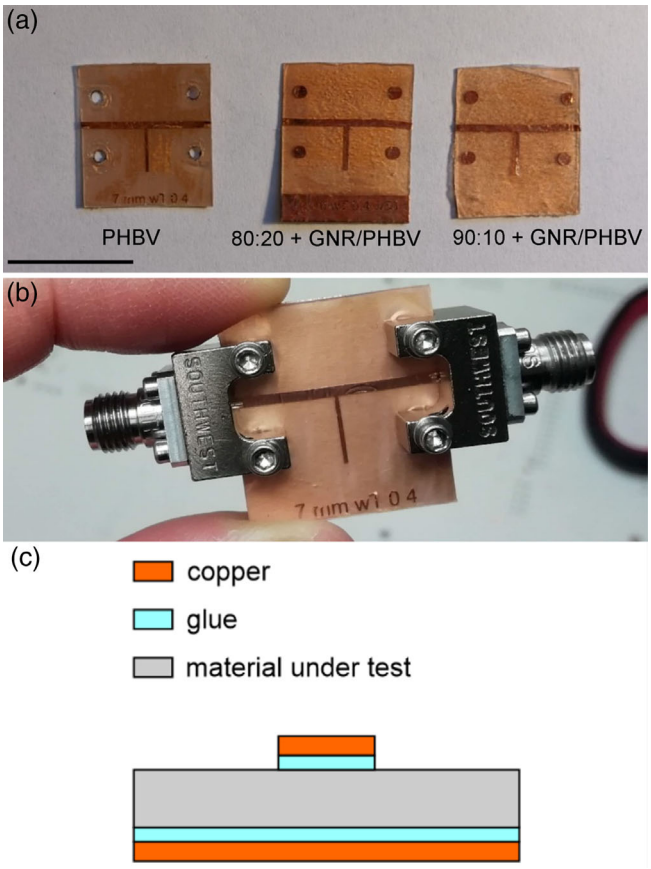

FIGURE 5 (a) Photo of the microstrip *T*-resonators implemented on the PHBV and RS-GNR/PHBV substrates. The scale bar indicates 20 mm, (b) Photo of the T-resonator implemented on the PHBV substrate between two end-launch connectors. The microstrip line used to connect the stub to the end-launch connectors has a length of 2 cm (1 cm for each side) and a width of 1 mm. The width of the stub is 400 μm, while its length is 7 mm, and (c) Schematic representation of the cross-section of the realized circuit. GNR, gold nanorods; PHBV, poly(3-hydroxybutyrate-*co*-3-hydroxyvalerate); RS, regenerated silk [Color figure can be viewed at wileyonlinelibrary.com]

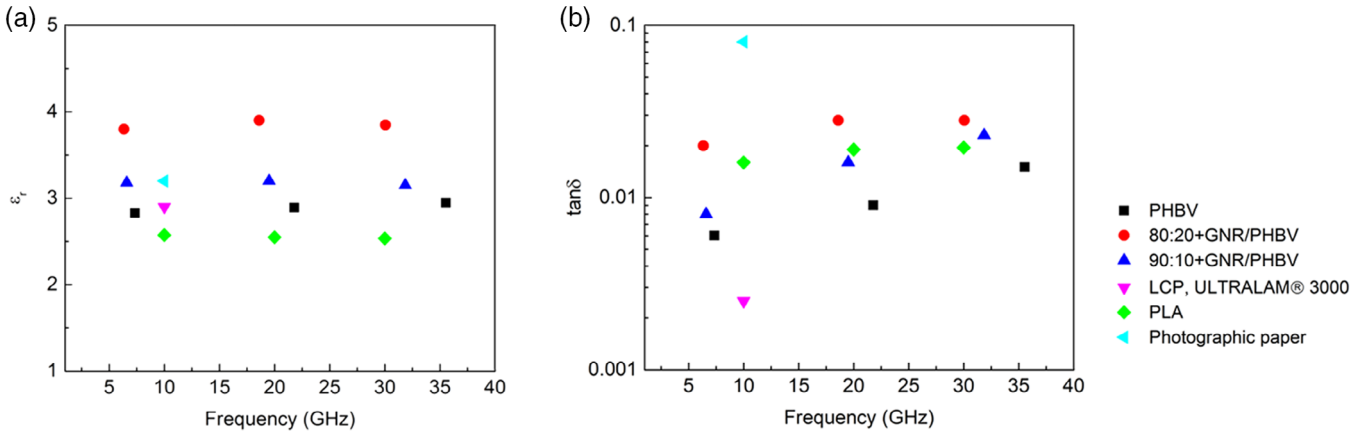

FIGURE 6 (a) Permittivity (ε_r) and (b) loss tangent (tanδ) versus frequency of PHBV and RS-GNR/PHBV substrates under test. The results are reported for comparison purpose with other materials representing the state of the art: liquid crystal polymer (LCP)-ULTRALAM® 3000,[37] polylactic acid (PLA)[38] and photographic paper.[26] LCP, liquid crystal polymer; PHBV, poly(3-hydroxybutyrate-*co*-3-hydroxyvalerate); PLA, polylactic acid; RS, regenerated silk [Color figure can be viewed at wileyonlinelibrary.com]

The obtained results of permittivity and loss tangent are shown in Figure 6(a) and (b), respectively. The results are also compared with other polymers reported in literature[25,34,35]: polylactic acid (PLA) and photographic paper are reported as examples of organic biodegradable polymers, while liquid crystal polymer (LCP) Ultralam© 3000 is considered as comparison for commercial flexible substrates. Specifically, the estimated constitutive parameters for the PHBV substrate are 2.83 for permittivity and 0.006 for the loss tangent at 7.35 GHz. Interestingly, these values in correspondence of the second resonance at 21.8 GHz (permittivity 2.90 and loss tangent 0.009) and third resonance at 35.55 GHz (permittivity 2.95 and loss tangent 0.015) are quite similar, which testifies the low dispersion of PHBV. Due to its low loss (PHBV loss tangent is lower than that of PLA and photographic paper in Figure 6(b)), PHBV qualifies as a good insulator, which can be suitable for microwave and millimeter-wave circuit design.

The RS-GNR/PHBV films show a higher loss due to the presence of the calcium chloride, (see Figure 6(b)). Indeed, the loss tangent of 80:20 + GNR/PHBV is higher than the loss tangent of 90:10 + GNR/PHBV, and in both cases it increases with frequency (that is particularly relevant for the sample 90:10 + GNR/PHB). Permittivity, instead, is quite stable varying the frequency for both RS-GNR/PHBV materials (the film with a higher concentration of calcium chloride has a higher permittivity). The loss tangent of the proposed films (in the range 0.008–0.028 at the considered frequencies) is comparable with the reported PLA values, which means that it is intermediate between photographic paper and LCP. The good dielectric properties of RS-GNR/PHBV films combined with their biocompatibility and piezoelectric properties make these materials extremely interesting for electronics, opening the door to new circuit designs and functionalities.

4 | CONCLUSIONS

In this paper, it has been reported a study on a hot-pressing method for obtaining RS with a low crystalline fraction. This allows the RS to be processed like a thermoplastic polymer. As proof of concept, we have fabricated by thermal adhesion a RS film on a bio-based polymer substrate and we have studied its piezoelectricity and the possibility of use as a force sensor. We have reported how the structure, mechanical properties, constitutive parameters, and piezoelectric characteristics are related to both the composition and thermal treatment. Since the use of piezoceramics has been widely studied in the field of regeneration of hard tissues, the present study could pave the way for the application of biodegradable piezoelectrics in regenerative medicine of soft tissues and production of smart electronics based on PHBV substrate.

ACKNOWLEDGMENTS

The authors acknowledge Dr Maria Cecilia Rossi and Dr Cinzia Restani for the technical support on NMR investigations (Interdepartmental Centre of Large Instruments, CIGS, University of Modena and Reggio Emilia, Italy). All authors are supported by the Italian Ministry of Education, University and Research (MIUR) under the PRIN Project "Development and promotion of the Levulinic acid and Carboxylate platforms by the formulation of novel and advanced PHA-based biomaterials and their

exploitation for 3D printed green-electronics applications" grant 2017FWC3WC_003.

CONFLICT OF INTEREST

There are no conflicts of interests to declare.

ORCID

Luca Valentini https://orcid.org/0000-0002-6803-5889
Micaela Degli Esposti https://orcid.org/0000-0002-4513-8527
Davide Morselli https://orcid.org/0000-0003-3231-7769
Paola Fabbri https://orcid.org/0000-0002-1903-8290

REFERENCES

[1] A. Koeppel, C. Holland, *ACS Biomater. Sci. Eng.* **2017**, *3*, 226.
[2] L. Shang, Y. Yu, Y. Liu, Z. Chen, T. Kong, Y. Zhao, *ACS Nano.* **2019**, *13*, 2749.
[3] B. Kundu, N. E. Kurland, S. Bano, C. Patra, F. B. Engel, V. K. Yadavalli, S. C. Kundu, *Prog. Polym. Sci.* **2014**, *39*, 251.
[4] C. X. Liang, *Polymer* **1992**, *33*, 4388.
[5] K. A. Trabbic, P. Yager, *Macromolecules* **1998**, *31*, 462.
[6] S. W. Ha, A. E. Tonelli, S. M. Hudson, *Biomacromolecules* **2005**, *6*, 1722.
[7] D. L. Rockwood, R. C. Preda, T. Yücel, X. Wang, M. L. Lovett, D. L. Kaplan, *Nat. Protoc.* **2011**, *6*, 1612.
[8] S. Ling, Q. Zhang, D. L. Kaplan, F. Omenetto, M. J. Buehler, Z. Qin, *Lab Chip* **2016**, *16*, 2459.
[9] S. Bittolo Bon, M. Rapi, R. Coletta, A. Morabito, L. Valentini, *Nanomaterials* **2020**, *10*, 179.
[10] L. G. P. Martins, Y. Song, T. Zeng, M. S. Dresselhaus, J. Kong, P. T. Araujo, *Proc. Nat. Ac. Sci.* **2013**, *110*, 17762.
[11] S. Bae, H. Kim, Y. Lee, *Nat. Nanotechnol.* **2010**, *5*, 574.
[12] B. D. Lawrence, M. Cronin-Golomb, I. Georgakoudi, D. L. Kaplan, F. Omenetto, *Biomacromolecules* **2008**, *9*, 1214.
[13] G. Chen, N. Matsuhisa, Z. Liu, D. Qi, P. Cai, Y. Jiang, C. Wan, Y. Cui, W. R. Leo, Z. Liu, *Adv. Mater.* **2018**, *30*(1–7), 1800129.
[14] Y. Qi, J. Kim, T. D. Nguyen, B. Lisko, P. K. Purohit, M. C. McAlpine, *Nano Lett.* **2011**, *11*, 1331.
[15] Y. Qi, T. D. Nguyen, P. K. Purohit, M. C. McAlpine, Stretchable piezoelectric nanoribbons for biocompatible energy harvesting. in *Stretchable Electronics* (Ed: T. Someya), Wiley-VCH, Weinheim, Germany **2012**, p. 111.
[16] T. Yucel, P. Cebe, D. L. Kaplan, *Adv. Funct. Mater.* **2011**, *21*, 779.
[17] M. Zhou, D. Yu, *Mol. Med. Rep.* **2014**, *10*, 508.
[18] P. Fabbri et al., Top emerging bio-based products, their properties and industrial applications. in *Directorate-General Research & Innovation (DG Research & Innovation)*, Ecologic Institute, Berlin **2018** Support to Research and Innovation Policy for Bio-based Products (BIO-SPRI) project, April 2017-June 2018, funding European Commission https://www.ecologic.eu/15776.
[19] A. Chen, *Chem. Soc. Rev.* **2009**, *38*, 2434.
[20] K. Rezwan, Q. Z. Chen, J. J. Blaker, A. R. Boccaccini, *Biomaterials* **2006**, *27*, 3413.
[21] G.-Q. Chen, Q. Wu, *Biomaterials* **2005**, *26*, 6565.
[22] M. Degli Esposti, F. Chiellini, F. Bondioli, D. Morselli, P. Fabbri, *Mater. Sci. Eng., C* **2019**, *100*, 286.
[23] Y. Ando, E. Fukada, *J. Polym. Sci., Polym. Phys.* **1984**, *22*, 1821.
[24] J. Jacob, N. More, C. Mounika, P. Gondaliya, K. Kalia, G. Kapusetti, *ACS Appl. Mater. Inter.* **2019**, *2*, 4922.
[25] S. Ke, H. Huang, L. Ren, Y. Wang, *J. of Appl. Phys.* **2009**, *105*, 96103.
[26] F. Alimenti, V. Palazzi, C. Mariotti, P. Mezzanotte, R. Correia, N. G. Carvalho, L. Roselli, *IEEE Microwave Mag.* **2018**, *19*, 48.
[27] A. Balfourier, N. Luciani, G. Wang, G. Lelong, O. Ersen, A. Khelfa, D. Alloyeau, F. Gazeau, F. Carn, *PNAS* **2020**, *117*, 103.
[28] C. Wan, C. R. Bowen, *J. Mater. Chem. A* **2017**, *5*, 3091.
[29] X. Hu, D. L. Kaplan, P. Cebe, *Macromolecules* **2006**, *39*, 6161.
[30] J.-W. Seo, H. Kim, K. H. Kim, S. Q. Choi, H. J. Lee, *Adv. Funct. Mater.* **2018**, *28*, 1800802.
[31] K. Yazawa, K. Ishida, H. Masunaga, T. Hikima, K. Numata, *Biomacromolecules* **2016**, *17*, 1057.
[32] H. Yuk, C. E. Varela, C. S. Nabzdyk, X. Mao, R. F. Padera, E. T. Roche, X. Zhao, *Nature* **2019**, *575*, 169.
[33] T. B. Reece, T. S. Maxey, L. A. Kron, *Am. J. Surg.* **2001**, *182*, S40.
[34] J. Li, A. D. Celiz, J. Yang, Q. Yang, I. Wamala, W. Whyte, B. R. Seo, N. Vasilyev, J. J. Vlassak, Z. Suo, D. J. Moone, *Science* **2007**, *357*, 378.
[35] B. P. Lee, P. B. Messersmith, J. N. Israelachvili, J. H. Waite, *Annu. Rev. Mater. Res.* **2011**, *41*, 99.
[36] E. Fukada, S. J. Takashit, *J. of Appl. Phys.* **1971**, *10*, 722.
[37] A.-V. H. Pham, M. J. Chen, K. Aihara, *LCP for Microwave Packages and Modules*, Cambridge University Press, Cambridge **2012**, p. 16.
[38] G. Boussatour, P. Cresson, B. Genestie, N. Joly, T. Lasri, *IEEE Microwave Wireless Compon. Lett.* **2018**, *28*, 374.

SUPPORTING INFORMATION

Additional supporting information may be found online in the Supporting Information section at the end of this article.

How to cite this article: Bittolo Bon S, Valentini L, Degli Esposti M, et al. Self-adhesive plasticized regenerated silk on poly(3-hydroxybutyrate-*co*-3-hydroxyvalerate) for bio-piezoelectric force sensor and microwave circuit design. *J Appl Polym Sci*. 2021;138:e49726. https://doi.org/10.1002/app.49726